Large-scale purification and characterization of recombinant *Pseudomonas* ceramidase: regulation by calcium[S]

Bill X. Wu, Christopher F. Snook, Motohiro Tani, Erika E. Büllesbach, and Yusuf A. Hannun[1]

Department of Biochemistry and Molecular Biology, Medical University of South Carolina, Charleston, SC 29425

Abstract **Ceramidases (CDases) hydrolyze ceramide to sphingosine (SPH) and fatty acid. *Pseudomonas* CDase (pCDase) is a homolog of mammalian neutral ceramidases and may play roles in disease pathogenesis. In this study, pCDase was cloned and expressed in *Escherichia coli* (*E. coli*). The expressed recombinant pCDase was solubilized by optimizing several factors, including culture medium, the concentration of isopropyl-β-thiogalactopyranoside (IPTG), temperature, and time of induction, which were identified to be critical for the optimal production of recombinant pCDase. The recombinant pCDase was purified using nickel-nitrilotriacetic acid affinity, phenyl-Sepharose, and Q-Sepharose column chromatography, which gave an overall yield of 0.45 mg/l purified protein of starting culture. The activity of the recombinant pCDase followed classical Michaelis-Menten kinetics, with optimum activity in the neutral pH range. Both the hydrolytic and the reverse activities of CDase were stimulated by calcium with an affinity constant (K_a) of 1.5 μM. Kinetics studies showed that calcium caused a decrease of K_m and an increase in V_{max} of pCDase. Calcium and D-*erythro*-sphingosine caused significant changes in the near ultraviolet circular dichroism (CD) spectra and the changes were inhibited in the presence of EGTA. These results identify important interactions between calcium and pCDase, which may play an essential role in the interaction of pCDase and its substrate.**—Wu, B. X., C. F. Snook, M. Tani, E. E. Büllesbach, and Y. A. Hannun. **Large-scale purification and characterization of recombinant *Pseudomonas* ceramidase: regulation by calcium. *J. Lipid Res.* 2007.** 48: **600–608.**

Supplementary key words circular dichroism • shphingolipid • ceramide

Sphingolipids, initially identified as important structural components of cell membranes, are now also recognized as vital regulators and mediators of many biological responses (1, 2). Among these bioactive species of sphingolipids, ceramide, sphingosine (SPH), ceramide-1-phosphate, and sphingosine-1-phosphate (S1P) have been extensively studied and identified as essential bioactive molecules in mediating cellular signaling pathways, including cell growth arrest, differentiation, apoptosis, chemotaxis, and inflammation (3–7). The levels and turnover of these bioactive molecules are controlled by several enzymes that play essential roles in the regulation of sphingolipid-mediated pathways.

Ceramidases (CDase, EC3.5.1.23) catalyze the cleavage of the N-acyl linkage in ceramide to form SPH and free fatty acid. Therefore, ceramidases play important roles in the regulation of the substrate ceramide, the immediate product SPH, and the further downstream metabolite S1P. According to the catalytic pH optima and primary sequence, CDases have been classified into three different groups: acid CDases, alkaline CDases, and neutral CDases. Genetic analysis reveals that the three CDase families are derived from different ancestral genes (8). Among the CDases, acid CDase is a lysosomal enzyme and its mutations cause the human disorder Farber's disease (9). Recently, several alkaline CDases were also cloned and characterized, including phytoCDase and dihydroCDase from yeast *Saccharomyces cerevisiae* (10, 11), a homolog of phytoCDase from human (12) and mouse alkaline ceramidase (13).

Neutral CDases (nCDases) have been cloned from many species, including, *Pseudomonas aeruginosa* (*P. aeruginosa*) (14), human (15), mouse (8), rat (16), *Drosophila melanogaster* (17), *Dictyostelium discoideum* (18), and zebrafish (19). Mammalian nCDases have also been purified to homogeneity and biochemically characterized from various tissues, e.g., mouse liver (20) and rat brain, kidney, and intestine (16, 21, 22). Mammalian nCDases appear to

Manuscript received 26 September 2006 and in revised form 29 November 2006.

Published, JLR Papers in Press, December 12, 2006.
DOI 10.1194/jlr.M600423-JLR200

Abbreviations: CD, circular dichroism; CDase, ceramidase; IPTG, isopropyl-beta-thiogalactopyranoside; LB, Luria-Bertani; nCDase, neutral ceramidase; NOE, *N*-oleoylethanolamine; *P. aeruginosa*, *Pseudomonas aeruginosa*; pCDase, *Pseudomonas* ceramidase; S1P, sphingosine-1-phosphate; SPH, sphingosine.

[1] To whom correspondence should be addressed.
e-mail: hannun@musc.edu

[S] The online version of this article (available at http://www.jlr.org) contains an additional figure.

play roles in cell proliferation and apoptosis by regulating the levels of ceramide, SPH, and S1P. For example, studies showed that retinal degeneration in *Drosophila* mutants can be rescued by targeted expression of human neutral CDase (23). In mesangial cells, nCDase was up-regulated by platelet-derived growth factor (24). Another report showed that nCDase also play roles in mediating the effects of advanced glycation end-products on cell proliferation (25). Dysfunction of nCDase causes impaired vesicle fusion and trafficking in the *Drosophila* nervous system (26).

nCDase has also been identified and characterized in two *Pseudomonas* strains (14, 27). *P. aeruginosa* is a gram-negative pathogen that can cause severe infection in patients with sepsis, cystic fibrosis, burns, or immunocompromised conditions. During *Pseudomonas* infection, ceramide has been proposed to play essential roles in host defense responses by reorganizing membrane rafts for internalization of the bacterium and in initiating immune signaling (28). Other studies provided evidence that the *Pseudomonas* ceramidase (pCDase) might play roles in hydrolysis of ceramide in skin in atopic dermatitis (29, 30).

Activity assays have shown that nCDase can catalyze both the hydrolysis of ceramide and its reverse reaction, the synthesis of ceramide, from SPH and fatty acid (31–33). The enzyme is regulated by anionic phospholipids and by calcium. However, the mechanism of calcium activation is unclear. Moreover, although extensive efforts have been made to investigate the biochemical properties of nCDase, no structural information is available.

In this study, recombinant pCDase was expressed and solublized by optimizing the expression conditions. The recombinant protein was purified and characterized. Importantly, calcium was shown to activate the enzyme with an affinity constant (K_a) of 1.5 μM, suggesting a relatively high affinity of interaction. By analyzing the circular dichroism (CD) spectrum of pCDase, the secondary structure was predicted, and near UV CD spectrum analysis also revealed significant interaction between calcium and pCDase. Therefore, this study not only provides knowledge for the regulation and biochemical properties of pCDase but also demonstrates that CD spectroscopy is a useful tool for the analysis of interactions between the enzyme, its substrates, and calcium activator.

EXPERIMENTAL PROCEDURES

Materials

All biochemicals were obtained from Sigma (St. Louis, MI) unless otherwise stated. D-*erythro*-C_{12}-NBD-ceramide and D-*erythro*-sphingosine were kindly provided by the Lipidomics Core Facility at the Medical University of South Carolina. NBD-C_{12} fatty acid was obtained from Molecular Probes (Eugene, OR). Anti-His_6 monoclonal antibody was obtained from Novagen (Madison, WI).

Cloning the pCDase

The DNA sequence encoding the *P. aeruginosa* PAO1 ceramidase was identified using BLAST software (http://www.ncbi.nlm.nih.gov/BLAST) against the *P. aeruginosa* PAO1 genome sequence (NC002516), using CDase cDNA sequence identified from *P. aeruginosa* strain AN17 (AB028646) (14). A Champion™ pET directional TOPO expression kit (Invitrogen, Carlsbad, CA) was used to clone and express the pCDase. Two oligonucleotides, a forward primer (5′-CACCATGTCACGTTCCGCATTCACCGC-3′) and a reverse primer (5′-CCTTGGCTGGAGCCCGCTAATGATGATGATGATGATGGGGAGTGGTGCCGAGCACCTCG -3′, the underlined sequences encoding His6-tag sequence), were synthesized. Using the above primers and *Pseudomonas* PAO1 genomic DNA as a template, the full-length coding sequence of pCDase (including the N-terminal signal peptide sequence) was amplified by Pfu-Ultra High Fidelity DNA polymerase and then cloned into pET101/D-TOPO vector (Invitrogen), directly followed by transformation of the construct into *E. coli* BL21 Star™(DE3) strain according to the manufacturer's instruction.

Expression of pCDase

For optimization of expression and induction conditions, the *E. coli* pCDase-BL21 was first grown in Luria-Bertani (LB) medium supplemented with 50 μg/ml ampicillin overnight, then transferred to M9 minimum or LB medium to optical density 600 of 0.1, and cells were grown to optical density 600 of about 0.5–0.8 (mid log) at 37°C. Induction conditions for expression of pCDase were optimized using different concentrations (0.1–1 mM) of isopropyl-beta-thiogalactopyranoside (IPTG), or different periods (3, 6 and 24 h) at different temperatures.

To detect the quantity and solubility of the expressed pCDase, the pCDase-BL21*E. coli.* cells were fractionated. The culture was first centrifuged at 3000 × *g* for 15 min to separate culture medium and cells. The pCDase-BL21 cell pellet was lysed by sonication and the unlysed cells were pelleted by centrifugation at 180 × *g* for 15 min. The supernatant was then centrifuged at 100,000 × *g* for 30 min to separate total membrane (insoluble) from soluble proteins. The supernatant was centrifuged again to remove any contaminant. The pellets were washed twice and then solubilized in 1% (w/v) Triton-X100. Equal amounts of protein from each fraction were subjected to SDS-PAGE and Western blot analysis using antibody specific to the His-tag as described previously (34).

After optimization, the induction condition for pCDase expression was finalized using 0.3 mM IPTG to pCDase-BL21 in M9 minimum medium for 24 h at 30°C before harvest.

Purification of recombinant *Pseudomonas* nCDase

Protein concentration was determined by the BCA method (Pierce, Rockford, IL) using BSA as a standard. Protein purification was peformed using a Pharmacia Akta-FPLC and columns purchased from GE health care. Cells were lysed by a combination of lysozyme treatment and sonication using a Model 500 sonicator (Fisher Scientific, Pittsburgh, PA). Cell pellets were resuspended (1 g/ml) in lysis buffer [0.02 M $NaPO_4$ (pH 7.2) 0.025 M imidazole, 0.5 M NaCl, 2 mM $MgSO_4$, 2 mM $CaCl_2$, 10 μg/ml DNase I 0.2 mg/ml lysozyme, protease inhibitor cocktail (Roche, Switzerland)] and incubated at 37°C for 1 h with gentle stirring. The lysate was then subjected to 10 s sonication nine times at a power setting of four with 1 min intervals. Unbroken cells and cell debris were removed by centrifugation at 40,000 × *g* for 30 min at 4°C. To precipitate nucleic acids, protamine sulfate was added to supernatants at a final concentration of 2.5 mg/ml. After another centrifugation at 40,000 × *g*, the resulting supernatant was loaded onto a Ni affinity column and eluted with buffer A [0.02 M $NaPO_4$ (pH 7.2) 0.5 M NaCl], and buffer B (buffer A plus 50 mM imidazole), with a linear

gradient from 0% to 30% of B. Fractions containing pCDase (as determined by SDS-PAGE and activity measurements) were pooled, adjusted to 1 M NaCl, and loaded onto a phenyl-sepharose column preequilibrated with buffer C, [50 mM Tris (pH 7.4)] containing 1 M NaCl. The proteins were eluted with a linear gradient of NaCl from 1 to 0 M. The pCDase fractions were pooled and applied directly to a Q-sepharose high performance column equilibrated with buffer D [50 mM Tris (pH 7.4)] and eluted with buffer D and C with a linear gradient from 0% to 20% of buffer C. The fractions containing pCDase, as determined by SDS-PAGE and activity assays, were pooled and subjected to further analysis.

CDase enzyme assays and biochemical characterization

Enzyme activity was measured using detergent/lipid mixed micelles with D-*erythro*-C_{12}-NBD-ceramide as a substrate at a concentration of 50 μM or 1.08 mol% in a 50 mM (pH 7.1) Tris buffer contained 1 mM $CaCl_2$, 0.3% (w/v) Triton X-100 final concentration, with a total volume of 100 μl. The enzymatic reaction was started by adding 1 ng of purified enzyme (unless otherwise stated). For the pH optimum determination, the substrate was dissolved in the following buffers: (pH 3.7–5.5) 50 mM acetate buffer, (pH 5.7–6.7) 50 mM MES buffer, (pH 6.3–7.3) 50 mM phosphate buffer, (pH 7.1–9.0) 50 mM Tris buffer, and (pH 8–10) 50 mM glycine-NaOH buffer. The enzymatic reaction was continued for 30 min at 37°C, and it was stopped by addition of chloroform/methanol (1:1). The organic phase was spotted onto TLC plates and analyzed as described previously (34).

To determine the calcium effects on the recombinant pCDase activity, 0.1 to 1 mM $CaCl_2$ were included in the 100 mM Tris (pH 7.1) buffer with 1 mM EGTA. The free Ca^{2+} concentrations were calculated using WEBMAXC_software (http://www.stanford.edu/~cpatton/webmaxc/webmaxcE.htm) (35). The kinetic parameters K_m and V_{max} were analyzed by Enzyme Kinetics software (SPSS).

The reverse CDase activity assays were performed as described (31) with modifications. Briefly, the substrates, 0.25 nmol of [^{3}H]palmitic acid, 9.75 nmol of unlabeled palmitic acid, and 10 nmol D-*erythro*-sphingosine were dried and then resuspended in 100 μl of reaction buffer[100 mM Tris buffer (pH 7.1) 0.2% (w/v) Triton X-100]; 1 ng recombinant pCDase was used for each reverse action, and the enzymatic reaction was conducted at 37°C for 2 h. The lipids were extracted and loaded on TLC plates as described above. The produced ceramide was visualized by autoradiography. The ceramide band and total remaining lipids were scraped separately for liquid scintillation counting. The percentage of ceramide synthesis for the reaction was calculated by comparing [^{3}H] ceramide band with total lipid.

CD measurements

The protein concentration of pCDase stock was determined by ultraviolet (UV) spectroscopy using an Olis Cary-15 spectrometer conversion in combination with a specific absorbance coefficient of 1.18 $mg^{-1}cm^2$ calculated by GCG peptidesort program (Genetics Computer Group, Inc, Madison, WI.). CD spectra were recorded using a Jasco J710 spectropolarimeter at ambient temperature at a resolution of 0.2 nm. All spectra were corrected for background by the subtraction of the buffer blank.

Far UV CD spectroscopy (190–250 nM) was measured in a cell of 0.1 cm pathlength. The *Pseudomonas* CDase solution was diluted to 0.28 mg/ml (~3.9 μM) in buffer containing 50 mM Tris (pH 7.4) and 40 mM octyl-β-glucoside. To test the effects of D-*erythro*-sphingosine or calcium on CD spectra, 120 μM D-*erythro*-sphingosine, 0.5 mM $CaCl_2$, or EGTA, was added to the buffer system, respectively. Ten spectra were averaged for each derivative. For spectra containing ultraviolet absorbing additives (i.e., D-*erythro*-sphingosine and EGTA), spectra were reported in the range of 197–250 nM, mean residue ellipticity ([θ]mrw) was calculated and helix content was estimated using the assumption that $[\theta]mrw_{222}$ for 100% helix is 40,000 (36).

For near UV CD spectroscopy (250–320 nm), a 1 cm pathlength cell was used, and forty spectra were averaged. Recombinant pCDase (0.28 mg/ml) was dissolved in 50 mm Tris (pH 7.4), 4 mM CHAPS, and the circular dichroism measured in the presence and absence of 120 μM D-*erythro*-sphingosine or *N*-oleoylethanolamine (NOE), in the presence of 0.5 mM $CaCl_2$ or EGTA. Spectra are displayed as molar circular dichroism (Δε).

RESULTS

Optimization of the pCDase expression

In order to examine structural and biochemical properties of pCDase, we established an expression system for large-scale purification. The full-length DNA coding sequence, encoding the pCDase, was cloned into pET101/D-TOPO vector under the control of the *lac* promoter. A His_6 tag was added to the C terminus to facilitate subsequent detection and isolation.

The pCDase-BL21 *E. coli* cells were first grown in LB medium and induced with 1 mM IPTG for 6 h. After fractionation of cell lysate, the majority of expressed pCDase was found in the insoluble fraction (the 100,000 × *g* pellet) using Western blot analysis (**Fig. 1A**). However, CDase activity was mainly in the soluble fraction (data not shown), suggesting that the majority of expressed pCDase was insoluble and largely inactive under these conditions. Thus, further optimization was necessary to increase the percentage of soluble protein and minimize the generation of inactive protein. First, different media were tried. As shown in Fig. 1A, expression induced in M9 minimum medium showed an approximate 3-fold increase of soluble protein when compared with expression in LB medium. Thus, M9 minimum medium was selected for the remaining optimization procedures. The optimum concentration of IPTG for the solubility of expressed pCDase was established next. As shown in Fig. 1B, the percentage of soluble pCDase increased with decreasing of IPTG concentration from 1 to 0.1 mM. Because 0.1 mM IPTG gave low expression, a concentration of 0.3 mM IPTG was employed for further optimization of induction time and temperature. Interestingly, when the induction temperature was decreased to 30°C for 24 h, the majority of recombinant pCDase became soluble while only trace amounts of pCDase were detected in the 100,000 × *g* pellet (Fig. 1C). Because the pCDase has been purified from medium as a secreted protein (32), we also tested for the recombinant pCDase in the medium. However, only trace amounts of pCDase were detected. Thus, the culture medium was not suitable for the purification of recombinant CDase under tested conditions. Therefore, by optimizing the culture and induction conditions, the expression of soluble and active protein was maximized, providing the basis for further purification and characterization.

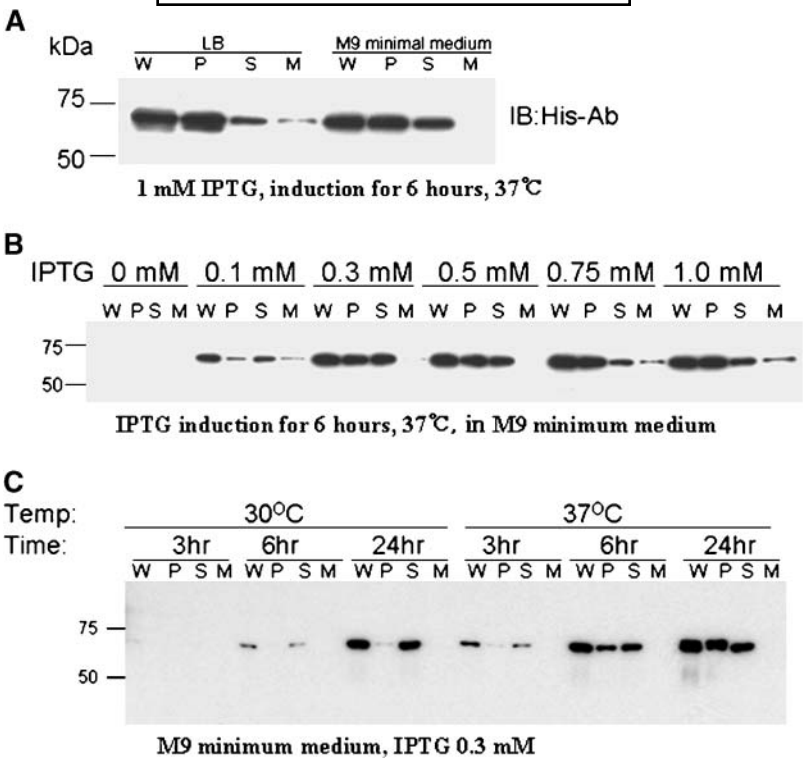

Fig. 1. Optimization of conditions for expression of *Pseudomonas* ceramidase (pCDase). BL21-pCDase cells were grown in M9 minimum or Luria-Bertani (LB) media and then induced with isopropyl-beta-thiogalactopyranoside (IPTG). Cell lysates were fractionated, and then 0.1% of each fraction as well as the culture medium were loaded to SDS-PAGE and analyzed by Western blot using His-tag antibody, as described in Experimental Procedures. A: Effects of LB or M9 minimum medium on solubility of recombinant pCDase. Cells were grown in LB or M9 minimum medium at 37°C and induced with 1 mM IPTG for 6 hr. B: IPTG effects on pCDase solubility. Ceramidase (CDase) expression was induced by different concentrations of IPTG for 6 h in M9 minimum medium at 37°C. C: Time and temperature effects on pCDase expression. Recombinant pCDase was induced by 0.3 mM IPTG for different periods in M9 minimum medium at 30°C or 37°C. M, culture medium; P, 100,000 × *g* pellet; S, 100,000 × *g* supernatant; W, whole lysate.

Purification of recombinant pCDase

The pCDase-BL21 cell pellet was lysed by a combination of lysozyme treatment and sonication. After precipitation of nucleic acids using protamine sulfate, the supernatant was subjected to three chromatographic purification steps (**Fig. 2A**). Thus, soluble fractions of crude cell-free extracts were first subjected to Ni affinity chromatography, followed by phenyl-sepharose chromatography, and finally by Q-sepharose high performance chromatography. Although the specific activity was not markedly increased by the latter steps (phenyl-sepharose and Q-FF columns), several impurities were removed as indicated by SDS-PAGE analysis (Fig. 2B). The purified pCDase migrated at about 70 kDa, matching the expected molecular mass as deduced from the cDNA sequence and previous reports on recombinant proteins (14, 27, 32). As judged by SDS-PAGE densitometry the enzyme obtained was >98% pure and had a high specific activity (2.7 μmol/min/mg), significantly higher than the purified recombinant pCDase of PAO1 reported previously (27). The recombinant pCDase was purified to near homogeneity with approximately 31% recovery of activity, summarized in **Table 1** and Fig. 2B.

Characterization of the expressed pCDase

The biochemical properties of purified recombinant pCDase were examined. As shown in **Fig. 3A**, the recombinant pCDase displayed a broad pH range with an optimum pH activity in the neutral range. The pH optimum is similar to those of mammalian nCDases.

Previous studies have suggested that pCDase is a calcium-dependent enzyme (14, 32). However, the relevant concentrations of calcium were not determined. Therefore, to determine the optimal concentration of free calcium for pCDase activity, free calcium concentrations were varied from 0.02 to 18.5 μM using EGTA/calcium buffers, and the concentrations of free calcium were calculated using MAXCHELATOR, a software established to determine free metal concentrations in the presence of chelators (http://www.stanford.edu/~cpatton/maxc.html) (35), As shown in Fig. 3B, pCDase activity increased with calcium concentrations with an apparent K_a of 1.5 ± 0.4 μM. The reverse CDase activity of pCDase was also activated by calcium with a similar K_a (Fig. 3D). To exclude the possibility of His-tag interference in the calcium effects on pCDase, we also partially purified native pCDase from

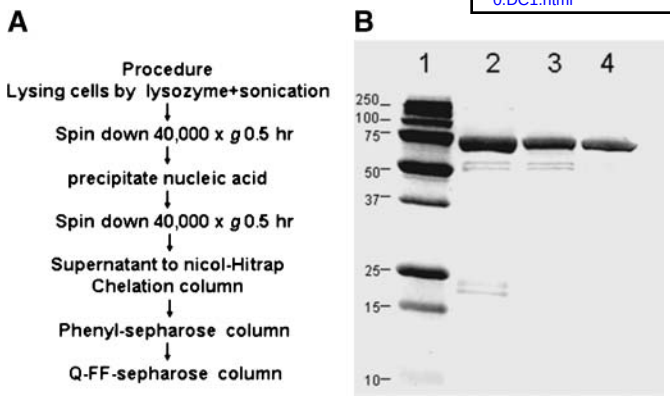

Fig. 2. Purification of pCDase. A: Procedures of purification of recombinant CDase. B: Electrophoretic analysis of purified pCDase from *E. Coli.* The same percentages (0.15%) of pooled fractions from purified proteins eluted from different columns were analyzed by gradient (4%–20%) SDS-PAGE and stained with Coomassie brilliant blue. Lane 1, MW marker; lane 2, pooled fractions from Ni column; lane 3, pooled fractions from Phenyl-sepharose column; lane 4, pooled fractions from Q-sepharose column.

200 ml culture medium of *P. aeruginosa* PAO1 using a diethylaminoethanol column as described previously (32), and the K_as for calcium were measured. The results (supplementary Fig. 1) showed that the native pCDase has the same K_a (1.5 μM) as the recombinant His-tagged pCDase, thus demonstrating that the His-tag did not interfere with the calcium effects on pCDase.

To determine the kinetic mechanisms of activation of pCDase by calcium, the effects of calcium on kinetic parameters were investigated at three different concentrations of free calcium (0.26, 0.7, and 18.5 μM). Interestingly, increasing calcium from 0.26 to 18.5 μM caused a decrease in the K_m of around 50%, and the V_{max} increased from 2.1 to 8.1 μmol/min/mg (Fig. 3C). This result suggests that calcium activates the pCDase in a mixed mechanism by enhancing both the substrate-enzyme affinity and catalytic capability.

TABLE 1. Purification of recombinant pCDase

Step	Protein	Activity	Specific activity	Recovery	Purification
	mg	*Units*	*Units/mg*	*%*	*Fold*
Cell lysates	2776	30.5	0.011	100.0	1.0
Supernatant	1250	23.7	0.019	77.8	1.7
Protamine sulfate supernatant	974	19.5	0.020	63.8	1.8
Nickel chelation column	7.5	14.4	1.9	47.1	174.4
Phenyl-sepharose	4.3	10.8	2.5	35.2	227.4
Q-sepharose	3.6	9.6	2.7	31.3	241.6

CDase was purified from eight liters of culture as described in Experimental Procedures. One enzyme unit was defined as the amount capable of hydrolyzing 1 μmol C12-NBD-ceramide/min at 37°C using D-*erythro*-C_{12}-NBD-ceramide as a substrate at a concentration of 50 μM or 1.08 mol% in a 50 mM (pH 7.1) Tris buffer contained 1 mM $CaCl_2$, 0.3% (w/v) Triton X-100 final concentration, with a total volume of 100 μl.

Far UV CD analysis

To acquire structural information and determine the conformational effects of calcium and substrates on the purified pCDase, CD spectroscopy was conducted (**Fig. 4**). The value of pCDase $[\theta]mrw_{222}$ was about 6000 deg $cm^2/dmol^{-1}$ corresponding to a 15% α helix content (36). A secondary structure prediction from the PSIPRED program (37) gave a similar prediction with 20% α-helices. These results suggest that the helical content of pCDase is likely in the range of 15–20%.

Calcium and SPH effects on CD spectra of pCDase

Because calcium activated pCDase, the effects of calcium on pCDase were investigated by CD spectroscopy. Initially, studies were performed in the far UV region; however, neither calcium nor EGTA affected the far UV spectra (Fig. 4A). The effects of the product of the reaction, D-*erythro*-sphingosine, which also serves as a substrate for the reverse reaction of the enzyme, were examined. As sphingolipids need to be solubilized for optimal delivery, a detergent needed to be chosen that dissolved sphingolipids but did not absorb UV light to allow for CD measurements. Specifically, triton X-100, used for activity studies, has a strong absorption band at 280 nm, and was therefore replaced by octyl-β-glucoside for far UV measurements and by CHAPS for near UV measurements. In either octyl-β-glucoside or CHAPS, pCDase retained full enzymatic activity while the background UV absorption was low. D-*erythro*-sphingosine in the presence and absence of calcium did not affect the CD in the far UV (Fig. 4B). Because far UV CD spectroscopy is primarily influenced by secondary structure, these results suggest that interactions between substrates or calcium with pCDase do not result in major changes in the secondary structure of pCDase.

On the other hand, changes in conformation may produce a difference in near UV CD spectra (320–250 nm), which are sensitive to changes in the tertiary structure of proteins (38). When the enzyme was incubated with calcium, it was found that calcium alone induced a clear change of the CD spectrum, affecting mostly the range from 250 to 265 nm (**Fig. 5A, B**). Therefore, calcium appears to modulate the overall conformation of pCDase but not its secondary structure.

In the presence of calcium, D-*erythro*-sphingosine caused further significant changes throughout the whole UV region (Fig. 5C, D). Comparing with the pCDase near UV spectra in the presence of calcium, maximum changes were still observed at 250–260 nm, while another broader region (270–310 nm) changed significantly with the maximum change at 288 nm (Fig. 5D). Moreover, the SPH effects on the pCDase UV CD spectra were significantly inhibited by the presence of EGTA (Fig. 5E, F), demonstrating a requirement for the free calcium. Taken together, these results show that calcium and SPH interact with the enzyme and result in significant changes in its tertiary structure.

Furthermore, we employed NOE, a ceramide analog and inhibitor of ceramidases, to determine its effects on near UV CD spectra of pCDase. Interestingly, NOE also induced

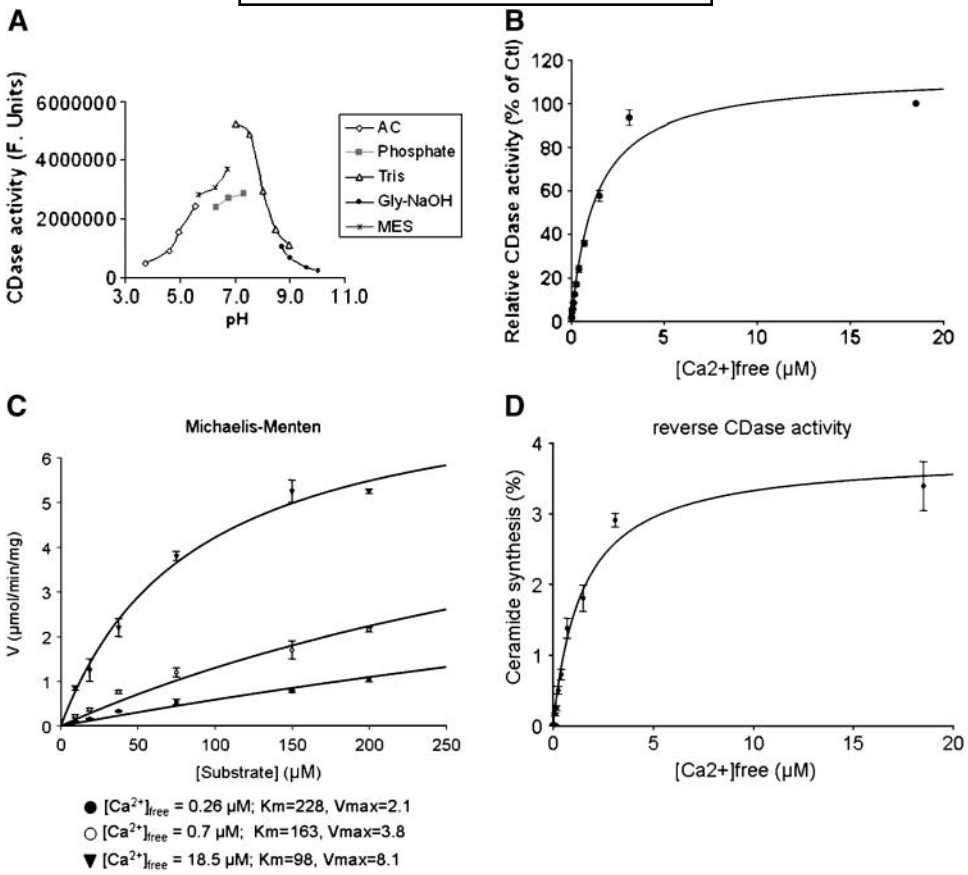

Fig. 3. Biochemical characterization of the purified recombinant pCDase activity. A: Determination of the pH optimum. The following buffers were used: (pH 3.7–5.5) 50 mM acetate buffer, (pH 5.7–6.7) 50 mM MES buffer, (pH 6.3–7.3) 50 mM phosphate buffer, (pH 7.1–9.0) 50 mM Tris buffer, and (pH 8–10) 50 mM glycine-NaOH buffer. The data are the averages of duplicates of at least two independent experiments. B: Calcium effects on CDase activity. CDase activity was analyzed in 100 mM Tris buffer, 1 mM EGTA and different concentrations of free calcium as described in Experimental Procedures. CDase activity at 18.5 μM $[Ca^{2+}]_{free}$ was set as control. C: Calcium effects on kinetics of CDase activity. Under three different calcium concentrations (0.26, 0.7, and 18.5 μM), Michaelis-Menten parameters for pCDase activity were acquired using 10–200 μM NBD-C12 ceramide as substrate. D: Calcium effects on the reverse activity. The percentage of ceramide synthesis for the reaction was calculated by quantifying [^{3}H] ceramide. The data in (B–D) are averages of triplicates and are representative of at least two independent experiments. F. Ctl, control; Units, arbitrary fluorescence units. Error bars represent standard deviation (n = 3).

significant changes of near UV CD spectra in the presence of calcium that were inhibited by EGTA (Fig. 5G, H). These results suggest that NOE may interact with pCDase directly.

DISCUSSION

In this study, pCDase was expressed, purified, and characterized. The induction conditions of the expression system were optimized, and the optimization resulted in the majority of the expressed pCDase in soluble form. The recombinant pCDase was also purified to apparent homogeneity using a three-column protocol. Calcium action on the enzyme and the mechanism for calcium activation of pCDase were studied using kinetic analysis and CD spectroscopy. These results revealed that calcium interacted with pCDase as a cofactor, and this interaction is essential for the activation of pCDase.

The current study identified a specific and relatively high-affinity interaction between neutral ceramidase and calcium. It has been shown that calcium enhances the activity of pCDase (14, 32). The current study focused on determining the mechanism of activation mechanism of pCDase by calcium. Analyzing the two activities of the recombinant enzyme, hydrolytic and reverse CDase activities, revealed a similar K_a of about 1.5 μM of the enzyme for free calcium (Fig. 3B, D). These results excluded the possibility that the activation occurs via calcium substrate interaction because that would have resulted in different K_as for these two types of activity assays using different substrates. Further kinetics analysis showed that free Ca^{2+} decreased the K_m of the enzyme toward its substrate ceramide (Fig. 3C), suggesting that calcium increases the affinity of the enzyme toward its substrate, probably through conformational changes. Interestingly, calcium also increased the V_{max} of pCDase toward its ceramide substrate,

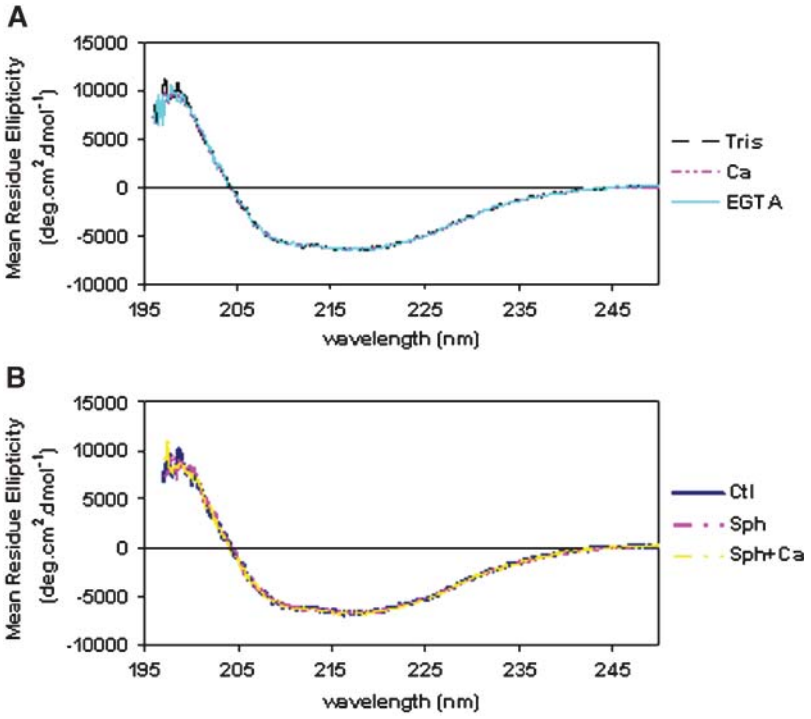

Fig. 4. Calcium, EGTA, and sphingosine (SPH) show no effects on far UV circular dichroism (CD) spectra of purified pCDase. CD spectra were measured in a cell of 0.1 cm pathlength. The pCDase was diluted to 0.28 mg/ml (~3.9 μM) in buffer containing 50 mM Tris, (pH 7.4) and 40 mM octyl-β-glucoside. All spectra were corrected for background by the subtraction of the buffer blank. A: Far UV CD spectra in control buffer (black line), with 0.5 mM $CaCl_2$ (purple line) or 0.5 mM EGTA (light blue line). B: Far UV CD spectra were measured in control buffer (dark blue line), with 120 μM SPH (purple line) or with SPH and 0.5 mM $CaCl_2$ (yellow line).

suggesting calcium can also modify the catalytic activity of the enzyme, suggesting effects of calcium on conformation of the enzyme and its optimal interaction with substrate.

These suggestions on conformational effects of calcium on the enzyme were probed directly using CD spectroscopy (Fig. 5). CD spectroscopy is an important tool to detect protein-protein and protein-ligand interactions, which typically do not produce a detectable difference in far UV CD spectroscopy but may produce a difference in near UV CD spectra. As shown in Fig. 5, calcium induced a significant spectral change around 253 nm. Further, in the presence of calcium, SPH caused significant changes throughout the near UV spectrum, suggesting additional conformational changes of pCDase upon interaction with SPH (substrate for the reverse reaction). The broad range implies that the chiral environment of multiple aromatic side chains must change upon substrate binding. Because pCDase contains 29 phenylalanines, 9 tryptophans, and 26 tyrosines, CD is not suitable to dissect the affected aromatic groups. For more precise measurement of substrate-induced conformational changes, X-ray crystallography would be the method of choice.

The strong requirement for activation of pCDase by calcium, and the high affinity of the interaction, raise possible pathophysiologic implications through regulation of *Pseudomonas* infections. Previous studies suggest that pCDase might play a role in skin diseases (29, 30). Interestingly, while *Pseudomonas* can cause serious infections in wounded skin, it cannot colonize or survive on healthy dry skin (39). In damaged skin, *Pseudomonas* is exposed to high levels of calcium in the extracellular fluid, which is unavailable on the surface of healthy skin. It is possible that this high level of extracellular calcium activates the secreted pCDase, which then hydrolyzes skin ceramides and results in exacerbation of dermatitis. Further, ceramide plays essential roles in host defense of *Pseudomonas* infections. After infection of mice with *Pseudomonas*, interruptions of generation of ceramide-enriched raft platform was shown to result in unabated inflammatory responses and septic death of mice (28). Thus, during infection with *Pseudomonas* in cystic fibrosis patients, extracellular calcium may activate pCDase, which could then interfere with the host defenses by degrading ceramide, possibly in rafts in outer plasma membrane of the airway epithelium.

Moreover, the high affinity of activation of pCDase by calcium with a K_a of around 1.5 μM raises the intriguing possibility that pCDase may be involved in the intracellular phase of *Pseudomonas* infection. While resting intracellular calcium is usually around 0.1 μM, many stimuli and agonists can rapidly raise the concentration to over 1 μM. This could then result in activation of pCDase which would decrease ceramide levels and increase those of SPH and S1P. These possibilities are worthy of further investigation.

A major goal for purification of recombinant pCDase in large amounts was to begin structural studies on the enzyme, as there is a significant paucity of structures of enzymes of lipid metabolism and other hydrophobic proteins. Previous studies have reported the purifications of recombinant CDases from different *P. aeruginosa* strains (14, 27). While the purification of pCDase from the growth medium most likely resulted in an active enzyme, the amount was low (27). The purification of refolded pCDase from inclusion bodies produced large amounts of protein, but the contamination of incorrectly folded protein could not be excluded and also the specific activity of the purified pCDase was low (27). In another study, CDase from *P. aeruginosa* strain AN17 was expressed and purified, but the yield was not specified (14). In our study, in order to

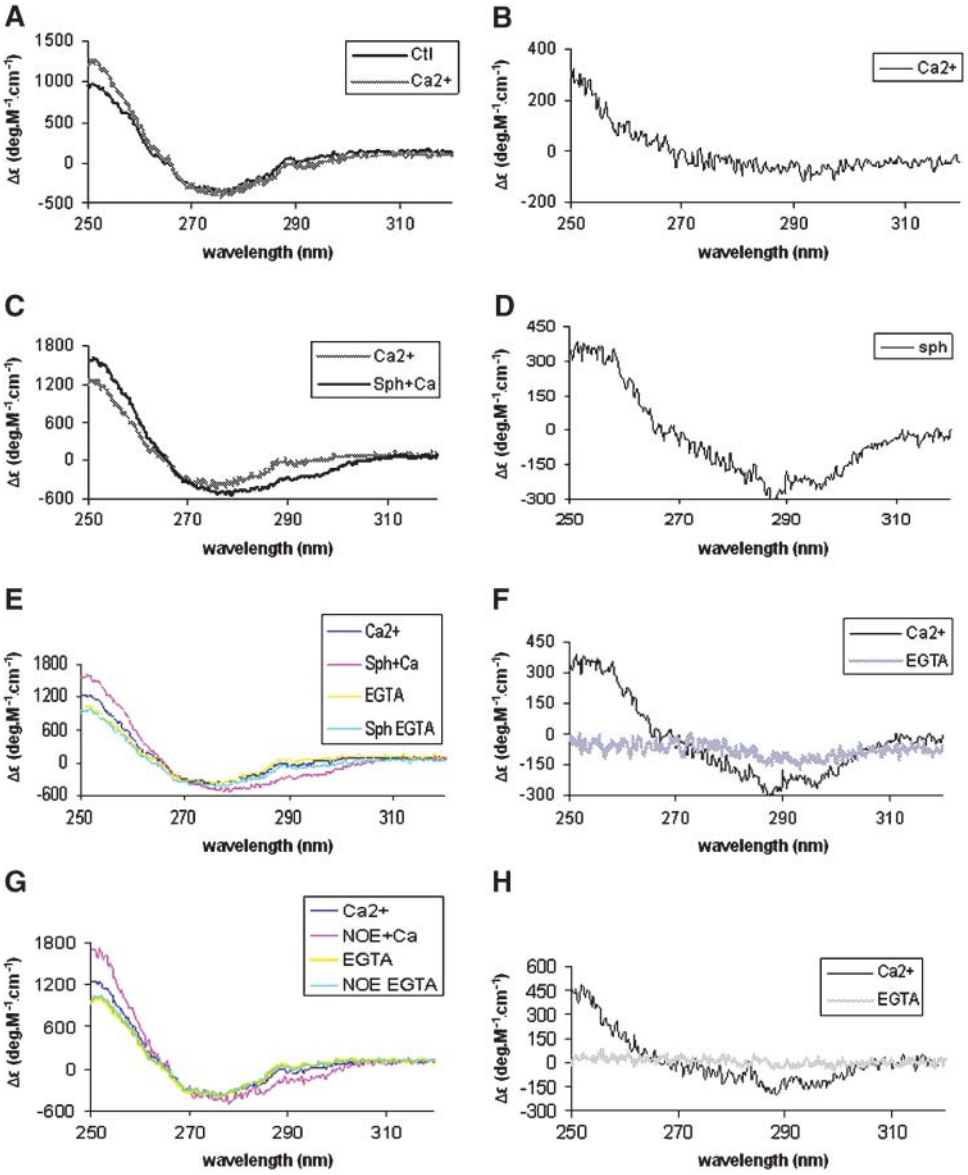

Fig. 5. Calcium, SPH, and *N*-oleoylethanolamine (NOE) induce changes in near UV CD spectra of purified recombinant pCDase. Near UV (250–320 nm) CD spectra were measured in 1 cm pathlength cell as described in Experimental Procedures. A, B: Ca^{2+} induced changes in near UV CD spectra of pCDase. A: CD spectra with or without adding $CaCl_2$ (0.5 mM). B: The difference of CD spectra with Ca^{2+}. The spectra were acquired by subtracting the pCDase spectra without Ca^{2+} from the spectra with 0.5 mM $CaCl_2$. C, D: SPH effects on near UV CD spectra in the presence of calcium. C: CD spectra of pCDase with or without 120 μM D-*erythro*-sphingosine in the presence of 0.5 mM Ca^{2+}. D: The difference of CD spectra with or without D-*erythro*-sphingosine in the presence of 0.5 mM Ca^{2+}. E, F: The effects of SPH on pCDase in the presence of calcium or EGTA. E: The near UV CD spectra of pCDase with or without D-*erythro*-sphingosine in the presence 0.5 mM EGTA or 0.5 mM $CaCl_2$. F: Comparison of the changes induced by SPH in the presence of 0.5 mM EGTA (gray line) or 0.5 mM $CaCl_2$ (black line). G, H: The effects of NOE on pCDase. G: The near UV CD spectra of pCDase with or without NOE in the presence EGTA or $CaCl_2$. H: Comparison of the changes induced by NOE in the presence of EGTA (gray line) or $CaCl_2$ (black line).

detect the expressed pCDase and facilitate the purification process, a C-terminal His-tag was added to the recombinant protein. As shown in Fig. 1, by optimizing the culture and induction conditions including medium, induction time, and concentration of IPTG, we successfully minimized the production of insoluble pCDase, providing the basis for the CD spectroscopic analysis. This approach to large-scale purification should also enable future crystallization studies, which necessitate large amounts of high quality purified protein.

In conclusion, although far UV CD spectrum analysis was previously employed in the study of secondary structures of sphingomyelinases from *Loxosceles* venom (40), this study is the first report using CD spectra to explore

enzyme-sphingolipid interactions, raising the possibility that CD spectroscopy could emerge as a valuable tool for studies of sphingolipid enzymes.

This work was supported by National Institutes of Health Grant CA-87584. The authors would like to thank Drs. Chiara Luberto and Fernando Alvarez-Vasquez, the DNA Sequencing Facility, and the Lipidomics Core at the Medical University of South Carolina for expert assistance.

REFERENCES

1. Hannun, Y. A., and L. M. Obeid. 2002. The Ceramide-centric universe of lipid-mediated cell regulation: stress encounters of the lipid kind. *J. Biol. Chem.* **277:** 25847–25850.
2. Ogretmen, B., and Y. A. Hannun. 2004. Biologically active sphingolipids in cancer pathogenesis and treatment. *Nat. Rev. Cancer.* **4:** 604–616.
3. Taha, T. A., Y. A. Hannun, and L. M. Obeid. 2006. Sphingosine kinase: biochemical and cellular regulation and role in disease. *J. Biochem. Mol. Biol.* **39:** 113–131.
4. El Alwani, M., B. X. Wu, L. M. Obeid, and Y. A. Hannun. 2006. Bioactive sphingolipids in the modulation of the inflammatory response. *Pharmacol. Ther.* **112:** 171–183.
5. Pettus, B. J., C. E. Chalfant, and Y. A. Hannun. 2002. Ceramide in apoptosis: an overview and current perspectives. *Biochim. Biophys. Acta.* **1585:** 114–125.
6. Modrak, D. E., D. V. Gold, and D. M. Goldenberg. 2006. Sphingolipid targets in cancer therapy. *Mol. Cancer Ther.* **5:** 200–208.
7. Chalfant, C. E., and S. Spiegel. 2005. Sphingosine 1-phosphate and ceramide 1-phosphate: expanding roles in cell signaling. *J. Cell Sci.* **118:** 4605–4612.
8. Tani, M., N. Okino, K. Mori, T. Tanigawa, H. Izu, and M. Ito. 2000. Molecular cloning of the full-length cDNA encoding mouse neutral ceramidase. A novel but highly conserved gene family of neutral/alkaline ceramidases. *J. Biol. Chem.* **275:** 11229–11234.
9. Sugita, M., J. T. Dulaney, and H. W. Moser. 1972. Ceramidase deficiency in Farber's disease (lipogranulomatosis). *Science.* **178:** 1100–1102.
10. Mao, C., R. Xu, A. Bielawska, and L. M. Obeid. 2000. Cloning of an alkaline ceramidase from Saccharomyces cerevisiae. An enzyme with reverse (CoA-independent) ceramide synthase activity. *J. Biol. Chem.* **275:** 6876–6884.
11. Mao, C., R. Xu, A. Bielawska, Z. M. Szulc, and L. M. Obeid. 2000. Cloning and characterization of a Saccharomyces cerevisiae alkaline ceramidase with specificity for dihydroceramide. *J. Biol. Chem.* **275:** 31369–31378.
12. Mao, C., R. Xu, Z. M. Szulc, A. Bielawska, S. H. Galadari, and L. M. Obeid. 2001. Cloning and characterization of a novel human alkaline ceramidase. A mammalian enzyme that hydrolyzes phytoceramide. *J. Biol. Chem.* **276:** 26577–26588.
13. Mao, C., R. Xu, Z. M. Szulc, J. Bielawski, K. P. Becker, A. Bielawska, S. H. Galadari, W. Hu, and L. M. Obeid. 2003. Cloning and characterization of a mouse endoplasmic reticulum alkaline ceramidase: an enzyme that preferentially regulates metabolism of very long chain ceramides. *J. Biol. Chem.* **278:** 31184–31191.
14. Okino, N., S. Ichinose, A. Omori, S. Imayama, T. Nakamura, and M. Ito. 1999. Molecular cloning, sequencing, and expression of the gene encoding alkaline ceramidase from Pseudomonas aeruginosa. Cloning of a ceramidase homologue from Mycobacterium tuberculosis. *J. Biol. Chem.* **274:** 36616–36622.
15. El Bawab, S., P. Roddy, T. Qian, A. Bielawska, J. J. Lemasters, and Y. A. Hannun. 2000. Molecular cloning and characterization of a human mitochondrial ceramidase. *J. Biol. Chem.* **275:** 21508–21513.
16. Mitsutake, S., M. Tani, N. Okino, K. Mori, S. Ichinose, A. Omori, H. Iida, T. Nakamura, and M. Ito. 2001. Purification, characterization, molecular cloning, and subcellular distribution of neutral ceramidase of rat kidney. *J. Biol. Chem.* **276:** 26249–26259.
17. Yoshimura, Y., N. Okino, M. Tani, and M. Ito. 2002. Molecular cloning and characterization of a secretory neutral ceramidase of Drosophila melanogaster. *J. Biochem. (Tokyo).* **132:** 229–236.
18. Monjusho, H., N. Okino, M. Tani, M. Maeda, M. Yoshida, and M. Ito. 2003. A neutral ceramidase homologue from Dictyostelium discoideum exhibits an acidic pH optimum. *Biochem. J.* **376:** 473–479.
19. Yoshimura, Y., M. Tani, N. Okino, H. Iida, and M. Ito. 2004. Molecular cloning and functional analysis of zebrafish neutral ceramidase. *J. Biol. Chem.* **279:** 44012–44022.
20. Tani, M., N. Okino, S. Mitsutake, T. Tanigawa, H. Izu, and M. Ito. 2000. Purification and characterization of a neutral ceramidase from mouse liver. A single protein catalyzes the reversible reaction in which ceramide is both hydrolyzed and synthesized. *J. Biol. Chem.* **275:** 3462–3468.
21. El Bawab, S., A. Bielawska, and Y. A. Hannun. 1999. Purification and characterization of a membrane-bound nonlysosomal ceramidase from rat brain. *J. Biol. Chem.* **274:** 27948–27955.
22. Olsson, M., R. D. Duan, L. Ohlsson, and A. Nilsson. 2004. Rat intestinal ceramidase: purification, properties, and physiological relevance. *Am. J. Physiol. Gastrointest. Liver Physiol.* **287:** G929–G937.
23. Acharya, U., S. Patel, E. Koundakjian, K. Nagashima, X. Han, and J. K. Acharya. 2003. Modulating sphingolipid biosynthetic pathway rescues photoreceptor degeneration. *Science.* **299:** 1740–1743.
24. Coroneos, E., M. Martinez, S. McKenna, and M. Kester. 1995. Differential regulation of sphingomyelinase and ceramidase activities by growth factors and cytokines. Implications for cellular proliferation and differentiation. *J. Biol. Chem.* **270:** 23305–23309.
25. Geoffroy, K., N. Wiernsperger, M. Lagarde, and S. El Bawab. 2004. Bimodal effect of advanced glycation end products on mesangial cell proliferation is mediated by neutral ceramidase regulation and endogenous sphingolipids. *J. Biol. Chem.* **279:** 34343–34352.
26. Rohrbough, J., E. Rushton, L. Palanker, E. Woodruff, H. J. Matthies, U. Acharya, J. K. Acharya, and K. Broadie. 2004. Ceramidase regulates synaptic vesicle exocytosis and trafficking. *J. Neurosci.* **24:** 7789–7803.
27. Nieuwenhuizen, W. F., S. van Leeuwen, R. W. Jack, M. R. Egmond, and F. Gotz. 2003. Molecular cloning and characterization of the alkaline ceramidase from Pseudomonas aeruginosa PA01. *Protein Expr. Purif.* **30:** 94–104.
28. Grassme, H., V. Jendrossek, A. Riehle, G. von Kurthy, J. Berger, H. Schwarz, M. Weller, R. Kolesnick, and E. Gulbins. 2003. Host defense against Pseudomonas aeruginosa requires ceramide-rich membrane rafts. *Nat. Med.* **9:** 322–330.
29. Kita, K., N. Sueyoshi, N. Okino, M. Inagaki, H. Ishida, M. Kiso, S. Imayama, T. Nakamura, and M. Ito. 2002. Activation of bacterial ceramidase by anionic glycerophospholipids: possible involvement in ceramide hydrolysis on atopic skin by Pseudomonas ceramidase. *Biochem. J.* **362:** 619–626.
30. Garcia-Sanchez, A., R. Cerrato, J. Larrasa, N. C. Ambrose, A. Parra, J. M. Alonso, M. Hermoso-de-Mendoza, J. M. Rey, and J. Hermoso-de-Mendoza. 2004. Identification of an alkaline ceramidase gene from Dermatophilus congolensis. *Vet. Microbiol.* **99:** 67–74.
31. El Bawab, S., H. Birbes, P. Roddy, Z. M. Szulc, A. Bielawska, and Y. A. Hannun. 2001. Biochemical characterization of the reverse activity of rat brain ceramidase. A CoA-independent and fumonisin B1-insensitive ceramide synthase. *J. Biol. Chem.* **276:** 16758–16766.
32. Okino, N., M. Tani, S. Imayama, and M. Ito. 1998. Purification and characterization of a novel ceramidase from Pseudomonas aeruginosa. *J. Biol. Chem.* **273:** 14368–14373.
33. Kita, K., N. Okino, and M. Ito. 2000. Reverse hydrolysis reaction of a recombinant alkaline ceramidase of Pseudomonas aeruginosa. *Biochim. Biophys. Acta.* **1485:** 111–120.
34. Galadari, S., B. X. Wu, C. Mao, P. Roddy, S. El Bawab, and Y. A. Hannun. 2006. Identification of a novel amidase motif in neutral ceramidase. *Biochem. J.* **393:** 687–695.
35. Bers, D. M., C. W. Patton, and R. Nuccitelli. 1994. A practical guide to the preparation of Ca2+ buffers. *Methods Cell Biol.* **40:** 3–29.
36. Kallenbach, N. R., and E. J. Spek. 1998. Modified amino acids as probes of helix stability. *Methods Enzymol.* **295:** 26–41.
37. McGuffin, L. J., K. Bryson, and D. T. Jones. 2000. The PSIPRED protein structure prediction server. *Bioinformatics.* **16:** 404–405.
38. Kelly, S. M., T. J. Jess, and N. C. Price. 2005. How to study proteins by circular dichroism. *Biochim. Biophys. Acta.* **1751:** 119–139.
39. Hojyo-Tomoka, M. T., R. R. Marples, and A. M. Kligman. 1973. Pseudomonas infection in superhydrated skin. *Arch. Dermatol.* **107:** 723–727.
40. de Andrade, S. A., M. F. Pedrosa, R. M. de Andrade, M. L. Oliva, C. W. van den Berg, and D. V. Tambourgi. 2005. Conformational changes of Loxosceles venom sphingomyelinases monitored by circular dichroism. *Biochem. Biophys. Res. Commun.* **327:** 117–123.